Applied Energy 205 (2017) 153–162

Contents lists available at ScienceDirect

Applied Energy

journal homepage: www.elsevier.com/locate/apenergy

A numerical investigation on methane combustion and emissions from a natural gas-diesel dual fuel engine using CFD model

Yu Li[a], Hailin Li[a,*], Hongsheng Guo[b], Yongzhi Li[c], Mingfa Yao[c]

[a] West Virginia University, Morgantown, WV 26506, USA
[b] National Research Council Canada, Ottawa, ON, Canada
[c] Tianjin University, Tianjin 300072, PR China

HIGHLIGHTS

- The CFD model with reduced PRF chemistry is able to simulate the combustion of methane in NG-diesel dual fuel engine.
- The main combustion process consumes 43–53% of methane.
- The post-combustion oxidation process consumes 17–29% methane.
- The unburned methane observed at EVO was distributed mainly at the center of the combustion chamber.

ARTICLE INFO

Keywords:
CFD model
Dual fuel engine
Methane emissions
Post-combustion oxidation

ABSTRACT

Natural gas (NG)-diesel dual fuel engines have been criticized for their high emissions of unburned methane. The past research on methane emissions from dual fuel engines has focused on the measurement of methane concentration in exhaust gases. The development of approaches capable of minimizing methane emissions requests the detailed spatial distribution of methane in-cylinder during the combustion and post combustion processes. However, it is difficult to experimentally measure the spatial distribution of methane in-cylinder.

This research presents a numerical study on the combustion process of a NG-diesel dual fuel engine using the computational fluids dynamics (CFD) model CONVERGE coupled with a reduced primary reference fuel (PRF) mechanism. The model was validated against the heat release process and the emissions of nitrogen oxide, methane and carbon monoxide measured in a single cylinder dual fuel engine. The validated CFD model was applied to investigate the combustion of methane and n-heptane and the spatial distribution of methane in the dual fuel engine. This is most likely the first attempt to visualize the spatial distribution of methane in dual fuel engines using CFD. The objective of this study is to numerically simulate the methane combustion process, especially the methane present outside the pilot spray, quantify the methane combustion in each combustion stage, and visualize the spatial methane distribution in cylinder. The results showed that the momentum produced by the pilot fuel injection and combustion pushed the combustion products of pilot fuel and methane within the pilot spray plume toward the unburned methane-air mixture. Such a movement enhanced the mixing of the hot combustion products and the relatively cold unburned methane-air mixture during the main combustion process and dominated the combustion of methane presented outside the pilot fuel spray plume. Based on the simulation results at a low load condition (4.05 bar), the main combustion process consumed 43–53% of the methane fumigated into the intake mixture. The post-combustion oxidation process consumed 17–29% of the intake methane, which was 36.2–51.8% methane that survived the main combustion process. In comparison, 27–35% methane emitted the engine without participating the combustion process. The unburned methane at exhaust valve opening was mainly observed at the center of the cylinder. In comparison, the contribution of the crevice and boundary layer around the cylinder liner to methane emissions was relatively small. The slip of methane through the dual fuel engines was due to the fact that the premixed mixture was too lean to support the propagation of the turbulent flame initiated by the pilot fuel and the lack of pilot fuel vapor reaching the center of the combustion chamber because of the geometric limitations of the fuel injection system and the reduced mass of pilot fuel injected into the cylinder. The approaches aiming to enhance the combustion of methane and

* Corresponding author.
E-mail address: hailin.li@mail.wvu.edu (H. Li).

http://dx.doi.org/10.1016/j.apenergy.2017.07.071
Received 14 February 2017; Received in revised form 4 July 2017; Accepted 18 July 2017
Available online 02 August 2017

minimize methane emissions from dual fuel engines should focus on those capable of increasing the volume of pilot fuel vapor formed after injected into the cylinder.

1. Introduction

Natural gas (NG) consisting of mainly methane has been recognized as a viable clean alternative fuel for its abundant resource, attractive features including producing less greenhouse gas (GHG) benefiting from the low carbon/hydrogen ratio of methane, low emissions of pollutants, especially particulate matter (PM), and high thermal efficiency. Natural gas can be burned as either the sole fuel in spark ignition (SI) engines [1,2] or as supplemental fuel in compression ignition (CI) diesel engines [3,4]. When burned in CI diesel engines, NG is usually fumigated into the intake mixture or directly injected into the cylinder early in the compression stroke, which forms a homogeneous NG-air mixture during the intake or early compression stroke. At the end of the compression stroke, a pilot of diesel fuel is injected into the hot NG-air-diluents mixture and serves as an ignition source. Prior to the injection of pilot diesel fuel, gaseous fuels have been well mixed with air and compressed to high temperatures, but usually not high enough to initiate the auto-ignition process of NG. After being injected into the hot bulk mixture, the pilot diesel is atomized, vaporized, mixed with the hot NG-air mixture, and ignited through compression ignition. The energy released by the pilot diesel fuel serves as an ignition source of the gaseous fuel. Detailed information about the dual fuel engine ignition and combustion process can be found in the literature [3,4].

Compression ignition dual fuel engines have been recognized as an attractive combustion mode for their potential to burn gaseous fuels at a thermal efficiency comparable to diesel engines and reduced PM emissions. Numerous researchers have examined the combustion process of dual fuel engines. For example, Karim [3] examined the heat release process derived from cylinder pressure and classified the heat release process of dual fuel combustion into three modes: (1) the ignition of the pilot fuel, which usually has higher reactivity than gaseous fuels fumigated into the intake mixture; (2) the concurrent combustion of diesel and NG presented within the diesel spray plume, (3) the combustion of a diesel free, NG-air mixture. The research conducted in the past decades has focused on the detailed experimental measurement of the impacts of engine speed [5,6], load [7–9], substitution ratio of NG [5,10], exhaust gas recirculation (EGR) [10,11], the mass of NG injected into intake manifold [12], and the amount of diesel fuel injected in each cycle [13] in the dual fuel engine combustion process. Recently, there has been increasing interest in examining the impact of pilot fuel injection timing and injection pressure on the combustion process and exhaust emissions from dual fuel engines [13–17]. The combustion process of NG was controlled by the mixing processes of the pilot fuel with the premixed charge (i.e. no flame propagation or bulk ignition) and whether or not the premixed NG-air mixture is too lean to support the propagation of the turbulent flames if initiated by pilot fuel. Past research on the combustion process of NG-diesel dual fuel engines has focused on the overall heat release process of NG and pilot diesel. In comparison, to the best of our knowledge, little research on the combustion process of gaseous fuels, such as methane, in dual fuel engines has been conducted. It is technically difficult to split the heat release of dual fuel engines to that of pilot fuel and gaseous fuel, respectively.

NG-diesel dual fuel engines have been criticized for their high emissions of unburned methane and carbon monoxide (CO). The methane emissions from dual fuel engines not only contribute to overall GHG emissions [18–20] but also cause a waste of energy [18,19]. Many researchers have investigated the methane emissions from NG-diesel dual fuel engines. For example, Karim et al. [21,22] measured the methane emissions from a single-cylinder NG-diesel dual fuel engine, and investigated the impact of engine load, methane concentration fumigated into the intake mixture, and diesel fuel injected in each cycle on the emissions of methane and CO. Egúsquiza et al. [7] investigated the effect of engine load, speed, substitution ratio on methane emissions and brake specific fuel consumption of a turbo-charged NG-diesel dual fuel engine with an aftercooler, and found that the methane emissions increased almost linearly with the increase in substitution ratio but decreased with the increase in engine load. With the concerns of fuel conversion efficiency in dual fuel engines, there has been interest in examining the combustion efficiency of methane fumigated into the intake mixture in NG-diesel dual fuel engines. For example, Gatts et al., [23] investigated the impact of engine load and the volumetric ratio of NG fumigated into the intake mixture on the emissions of methane and CO from a turbo-charged heavy-duty NG-diesel dual fuel engine. The emissions of methane, CO, and carbon dioxide (CO_2) and the flow rates of fuels and air were further processed to derive the combustion efficiency of methane with the following two assumptions: (1) the methane emitted from the dual fuel engine was that added into the intake mixture; and (2) the CO emissions above that of pure diesel operation was due to the incomplete combustion of methane while disregarding the possibility of incomplete combustion of diesel and other hydrocarbons in natural gas. The lowest combustion efficiency observed at low (10%) load operation was about 65%. The maximum combustion efficiency observed at 70% load was about 95%, similar to that of SI NG engines. It is evident from these early investigations that the improvement of methane combustion efficiency of dual fuel engines at low load is one of the key challenges for the wide application of dual fuel engines especially when low load operation is frequently involved.

The contribution of unburned methane to GHG emissions and the desire to further improve the efficiency of dual fuel engines have raised researchers' interest to understand the mechanism for methane to survive the combustion process and slip through the combustion chamber without participating in combustion. Some researchers tried to investigate the combustion process of dual fuel engines using advanced combustion diagnostic technologies and managed to measure the propagation of flames through the premixed mixture of NG and air. For example, Dronniou et al. [24] investigated the dual fuel engine combustion process using a single-cylinder optical research engine representing typical modern, light-duty diesel engines. A high-speed digital camera recorded time-resolved combustion luminosity. An intensified charge-coupled device (CCD) camera was used for single-cycle OH* chemiluminescence imaging. The propagation of the turbulent flame through the diesel fuel free bulk gas (premixed NG-air mixture) was observed when the NG-air mixture was richer than the lean flammability limit [24]. However, the NG-air mixture leaner than the flammability limit was not able to support the propagation of the flames initiated by the pilot diesel fuel [24,25]. Nithyanandan et al. [26] visualized the flame propagation process in a NG-diesel dual fuel engine with optical access using a color high-speed camera. The combustion in different zones representing the lean premixed methane-air mixture and pilot fuel diffusion combustion was distinguished using the temporally resolved natural luminosity imaging. The impact of fuel injection strategy and equivalence ratio of the premixed NG-air mixture on the flame propagation through the premixed NG-air mixture was also examined. Combining the natural luminosity image with the heat release rate (HRR) helped to better understand the overall heat release process and the burning of pilot and gaseous fuels. The research identified the multi-pulse fuel injection strategies as a promising and effective strategy capable of enhancing the flame propagation toward the center of the combustion chamber, which was usually not burned with a single pulse injection strategy [26]. However, these technologies were

not able to measure the spatial distribution of methane in-cylinder, especially the interface where hot combustion products mix with the cold unburned NG-air mixture. The spatial distribution of methane in-cylinder and percentage of the methane consumed in each combustion stage and that left unburned has not been quantified. Liu et al. [27] discussed the pathways for methane to be consumed in a heavy-duty NG-diesel dual fuel engine, including: (1) the concurrent combustion of methane with diesel fuel within the diesel spray plume; (2) the consumption of methane by the propagating flame initiated by pilot diesel when the methane-air mixture is rich enough to support the propagation of turbulent flames; (3) the post-combustion oxidation of methane that survived the main combustion process but later on mixed with the hot combustion products. The methane that survived the main combustion process and post-combustion oxidation process would slip through the combustion chamber and leave the engine as unburned methane; (4) the methane fumigated can also be burned through auto-ignition, which may occur early in the combustion stage around the top dead center (TDC), but auto-ignition usually must be suppressed as it will lead to the onset of knock [28].

The research on the spatial distribution of methane in-cylinder, quantification of the percentage of methane burned in each combustion stage and the mechanism for methane to survive the combustion process is of critical importance for the development of technical approaches optimizing the dual fuel engine combustion process and minimizing methane emissions. However, because of the difficulty in experimental techniques, the spatial distribution of methane within the combustion chamber and the mechanism for methane to survive the combustion process in dual fuel engines have never been experimentally identified.

The computational fluids dynamics (CFD) modeling has been recognized as a platform for the investigation of the combustion process of internal combustion engines, especially compression ignition engines involving diffusion combustion. A CFD model coupled with a chemical kinetic mechanism has been applied to simulate the diesel injection process, the formation of diesel-NG-air mixture, oxidation of diesel and methane, and the formation of pollutants including mainly nitrogen oxide (NO_x) in NG-air dual fuel engines [29–32]. For example, Liu et al. [29] simulated the combustion characteristics of a dual fuel engine with a swirl chamber using the CFD software KIVA-3 as a platform. The model coupled with fuel chemistry was able to predict the combustion process and the formation of NO_x in a light-duty 4-cylinder NG-diesel dual fuel engine. Nieman et al. [30] numerically investigated the operation of a NG-diesel dual fuel engine operated on the reactivity controlled compression ignition (RCCI) mode using a KIVA 3V CFD code and were able to simulate the formation of soot, NOx, CO, and unburned hydrocarbon (UHC) emissions. Maghbouli et al. [31] numerically investigated the impact of multi-pulse pilot fuel injection strategies on the combustion process of a dual fuel engine. The impact of injection timing of the 1st and 2nd injection pulse on the combustion process, exhaust emissions and the contribution of diesel to the total energy were simulated. It was evident that the previous numerical studies on dual fuel engines have focused on the overall heat release process and formation of pollutants in cylinder. In comparison, the consumption of methane in each combustion stage and mechanism for methane to survive the main combustion and the post-combustion oxidation process have never been reported by any numerical study. The knowledge needed in evaluating the extent of success of engine operation and control strategy in minimizing methane emissions is not available.

This research investigated the combustion process of methane in a single cylinder NG-diesel dual fuel engine using a 3D CFD code CONVERGE coupled with a reduced primary reference fuel (PRF) mechanism including the oxidation of methane. The model was validated against experimental data including the cylinder pressure, HRR, and exhaust emissions of NO_x, methane and CO. The validated model was applied to investigate the consumption of methane during the main and post-combustion process. The mechanism for methane to survive the main and post-combustion oxidation process is examined. The spatial distribution of methane in cylinder during the compression process, main combustion process, and post combustion process is examined. The combustion process of methane and pilot fuel is further processed to develop the percentage of methane consumed in each combustion stage. The percentage of methane that survived the main combustion and post-combustion process can be adopted as criteria in evaluating the extent of success of pilot fuel injection strategies in enhancing the combustion of premixed gaseous fuels and minimizing the methane emissions from dual fuel engines.

Following the introduction section that provides a detailed literature review and the objective of the research, a section to introduce the experimental facility, numerical model, fuel chemistry and other sub-models adopted is provided. Then the paper discusses and analyzes the simulation results, aiming at the combustion of methane in a dual fuel engine, the spatial distribution of methane in cylinder during the combustion process and the percentage of methane burned in each combustion stage. Finally, conclusions are provided.

2. Experimental setup and numerical simulation model

2.1. Experimental set-up

The experiments were conducted in a single cylinder, 4-valve, caterpillar diesel engine with a compression ratio of 16.25, bore of 137.2 mm, and stroke of 165.1 mm. The engine test cell was configured to simulate the operation of a turbocharged heavy-duty diesel engine. The detailed specification of the engine, dynamometer, data acquisition system, and exhaust gas analyzer can be found in the literature [33]. The engine was converted by the National Research Council Canada (NRC) to operate in the NG-diesel dual fuel mode. In this research, NG was added to the intake air using a port-fuel NG injector installed between the intake surge tank and intake valve. The pilot diesel was directly injected into the cylinder using a common-rail fuel injection system at 525 bar. The diesel injector has 6 injection holes of diameter 0.23 mm and is installed at the center of the cylinder head. The injection spray angle was 65°. In this research, the engine was operated at an engine speed of 910 rpm, and a brake mean effective pressure (bmep) of 4.05 bar, a typical low load operation condition featured with low methane combustion efficiency. The gaseous fuel used was pipeline natural gas consisting of 95.80% methane, 2.34% ethane, 0.19% propane, 0.98% N_2, 0.64% CO_2 and traceable high hydrocarbons [33]. Tables 1 and 2 show the main parameters and operating conditions simulated in this study. Table 3 shows the mass flow rate of diesel fuel and NG at each case tested. The energy contribution of NG was reported as the ratio of energy of NG relative to total energy consumed. For example, 25% NG represents a case with 25% energy provided by NG and 75% energy provided by pilot fuel.

Table 1
Basic engine parameters.

Parameter	Value
Basic engine model	Caterpillar 3401
Parent engine	Caterpillar 3400 series
Number of cylinder	1
Bore × stroke	137.2 mm × 165.1 mm
Compression ratio	16.25:1
Displacement	2.44 L
Number of valve	4
Combustion chamber type	Quiescent
Diesel fuel injection type	Direct injection
Diesel fuel injector	Ganser CRS AG
National gas injection type	Port injection
Natural gas injector	AFS Gs60 injectors
Maximum power output	74.6 kW (@2100 rpm)

Table 2
Engine operation parameters.

Engine speed	910 rpm
Engine load	4.05 bar bmep
Intake temperature	40 °C
Intake pressure	105 kPa
EGR rate	0%
Diesel injection pressure	525 bars
Injection timing	−7 °CA ATDC

Table 3
The mass of diesel and NG consumed each cycle at each case.

Cases tested		Diesel fuel	Natural gas		
		Mass, mg/cycle	Mass, mg/cycle	Vol. conc. in intake mixture (%)	NG contribution to total fuel energy (%)
Case 1	0% NG	66.2	0.0	0.00	0
Case 2	25% NG	49.7	15.5	1.33	25
Case 3	50% NG	34.8	32.2	2.72	50
Case 4	75% NG	18.1	50.9	4.21	75

2.2. Numerical simulation model

The simulation model used is the 3D CFD software CONVERGE [34]. The diesel fuel was represented by n-heptane. NG was represented by methane. The fuel chemistry used was a reduced PRF mechanism consisting of 45 species and 142 reactions [35]. The physical property of diesel fuel was represented by tetradecane ($C_{14}H_{30}$) to simulate the spray development, atomization, vaporization and the mixing of n-heptane with air. Table 4 shows the list of sub-models applied for simulation, which had been validated by Yang et al. [36] for a gasoline/diesel dual fuel combustion study. The spray-wall interaction was simulated using an O'Rourke model [37]. An adaptive mesh generation method with up to 300,000 grids was applied. Fig. 1 shows an example of the mesh generated. The simulation started from the intake valve closing (IVC) with the assumed homogeneous mixture of natural gas, air, and residual gas and completed at the exhaust valve opening (EVO). The pressure, temperature, and composition of bulk mixture were calculated with the cylinder pressure and temperature at the end of the exhaust stroke. The mass and concentration of the air-fuel mixture consumed each cycle was calculated using experimental data. The simulation data was processed to examine the mechanism for methane to survive the main and post-combustion process, the spatial distribution of methane in-cylinder, and the percentage of methane consumed in each combustion stage.

3. Results and discussion

The model was validated against experimental data measured at the NRC. As shown in Fig. 2, the simulated cylinder pressure and HRR agree well with experimental data measured with NG contributing up to 75% of the total energy consumed. The model was also able to reasonably predict the trend of NO_x, CO and methane emissions, as shown in Fig. 3. The quantitative difference between the measured and simulated emissions might be due to the imperfect pilot fuel spray model, the representation of diesel fuel using n-Heptane, the reduced fuel chemistry, and the presence of ethane in NG which was not accounted for in the simulation model due to the limitation of fuel chemistry. The evaluation of the simulated methane and CO emissions at EVO other than exhaust gas might also contribute to the difference between the simulated methane and CO emissions and experimental data. Although the CFD model over-predicted the methane emissions and under-predicted the CO emissions (shown in Fig. 3), the predicted sum of the mass of CO and methane at EVO agreed well with the experimental data, as shown in Fig. 4. It is evident that the CFD model is able to reasonably predict the percentage of methane burned in a dual fuel engine.

Fig. 5 shows the percentage difference between the predicted and measured peak cylinder pressure (PCP) and CO + CH_4 emissions with experimental data. The maximum difference between the predicted and measured PCP is 2.5%. The maximum difference between the measured and predicted emissions of CO + CH_4 is 12.0%, which is observed at 75% NG. The difference between the predicted and measured CO + CH_4 emissions in the other three cases is relatively low (within 7%). It is evident that the CONVERGE CFD model with a reduced PRF mechanism is able to reasonably simulate the combustion process of methane in the dual fuel engine tested. In this research, the validated CFD model is applied to evaluate the combustion process of n-heptane and methane in each combustion stage in this dual fuel engine.

Fig. 6 shows the simulated evolution of n-heptane spray, the distribution of temperature, equivalence ratio (ER), and methane in a cut-plane in the middle of the injection spray for the 25% NG case. In this research, the ER was calculated using the concentration of fuel and O_2 without accounting for CO_2 and H_2O formed through combustion of the pilot and gaseous fuel. With the development of the spray plume, the ER inside the n-heptane spray plume is found to first gradually increase accompanied with the injection of pilot fuel but then decrease due to the atomization and vaporization of n-heptane, and mixing with the methane-air mixture. The continued increase in ER within pilot fuel spray, especially after the consumption of n-heptane, is due to the consumption of O_2 during the combustion process of n-heptane and methane within the spray plume. The concentration of methane and the temperature inside the spray are noted to increase from −2.5 to 0.1 °crank angle (CA) after top dead center (ATDC). This is due to the formation of methane during the oxidation of n-heptane. As shown in Table 3, the molar fraction of methane in the intake mixture at 25% NG is 1.33%, which is much leaner than the lean flammability limit of methane [25]. Accordingly, not all of the methane present outside the n-heptane spray plume can be burned due to the lack of flame propagation. With the combustion of methane in the rich mixture featured with ER > 1, the ER value would further increase due to the consumption of O_2. In comparison, the ER of the lean fuel mixture (ER < 1) would gradually decrease to zero (complete combustion) with the consumption of fuel as there is excess O_2 present. The temperature distribution shows that ignition is first observed at the periphery of the n-heptane plume where n-heptane and air are sufficiently mixed.

Fig. 7 shows the variation of cylinder pressure, HRR, and average molar fraction of n-heptane, methane, CO, OH, CH_2O and H_2O_2 with the change in crank angle for the 25% NG case. N-heptane evolution endures a two stage consumption representing the transfer from the low temperature oxidation to the negative temperature coefficient (NTC) region. The production of OH is accompanied with the consumption of n-heptane after about −2.3 °CA ATDC, which is recognized as the start of high temperature combustion (HTC) of the premixed n-heptane/air/methane. Active radicals such as CO, CH_2O, and H_2O_2, are found to gradually increase prior to the start of HTC following the injection of pilot fuel. The premixed combustion starts from −2.3 °CA ATDC and lasts until 1 °CA ATDC during which the n-heptane-methane-air mixture at the periphery of the n-heptane plume burns. The diffusion

Table 4
List of sub-models used in the simulation.

Phenomenon	Model	Reference
Spray-wall interaction	O'Rourke	[37]
Spray breakup	Hybrid KH-RT	[38]
Droplet collision	NTC collision method	[39]
Turbulence	Renormalized k–ε model	[40]

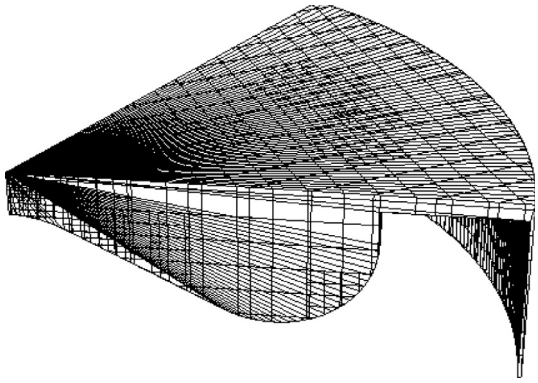

Fig. 1. Computational mesh at TDC.

combustion of n-heptane starts at 1 °CA ATDC and lasts until 4.5 °CA ATDC as indicated by the complete consumption of n-heptane. During this period, the production of the intermediate combustion products such as CO is accompanied with the simulated production of methane. The radicals such as H_2O_2 and CH_2O are found to gradually decrease to very low values with the consumption of n-Heptane. Methane is mainly consumed during the late diffusion combustion after the completion of n-heptane combustion. The continued release of heat after complete consumption of n-heptane is due to the combustion of methane only. The oxidation of methane after the complete combustion of n-heptane is accompanied with high concentrations of CO and OH. In comparison, the concentrations of CH_2O and H_2O_2 observed after the complete combustion of n-heptane is relatively small compared with their peak values.

The combustion of methane and geometric location of the survived methane within the bulk gas are examined by evaluating the distribution of temperature (over 1800 K representing region involving combustion of n-heptane, and methane), combustion products such as CO_2,

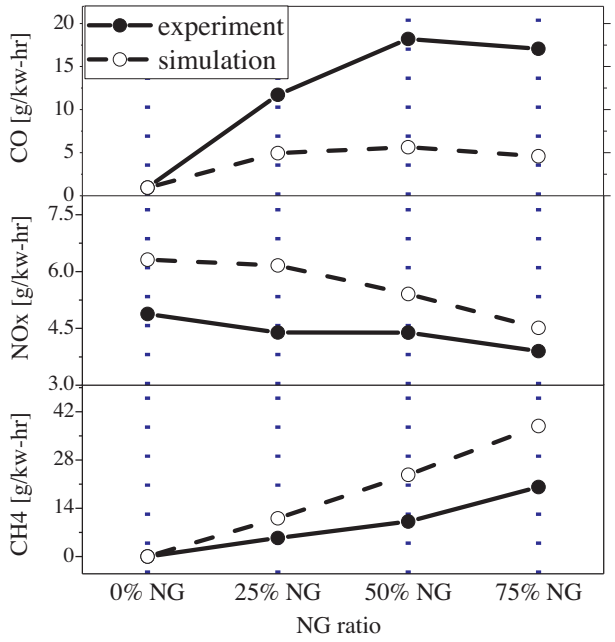

Fig. 3. Comparison of simulated CO, NOx and CH_4 emission with experimental data.

concentration of O_2 and methane in the bulk gas. Fig. 8 shows the velocity field from injection and hot combustion products represented by the region where T > 1800 K. It should be noted that the color of the arrow represents the value of the velocity of bulk gas movement. The momentum of bulk gas created by the spray jet, piston movement, and combustion pushed the hot combustion products toward the unburned methane-air mixture. The mixing between the hot combustion products and the cool methane-air mixture increases the temperature,

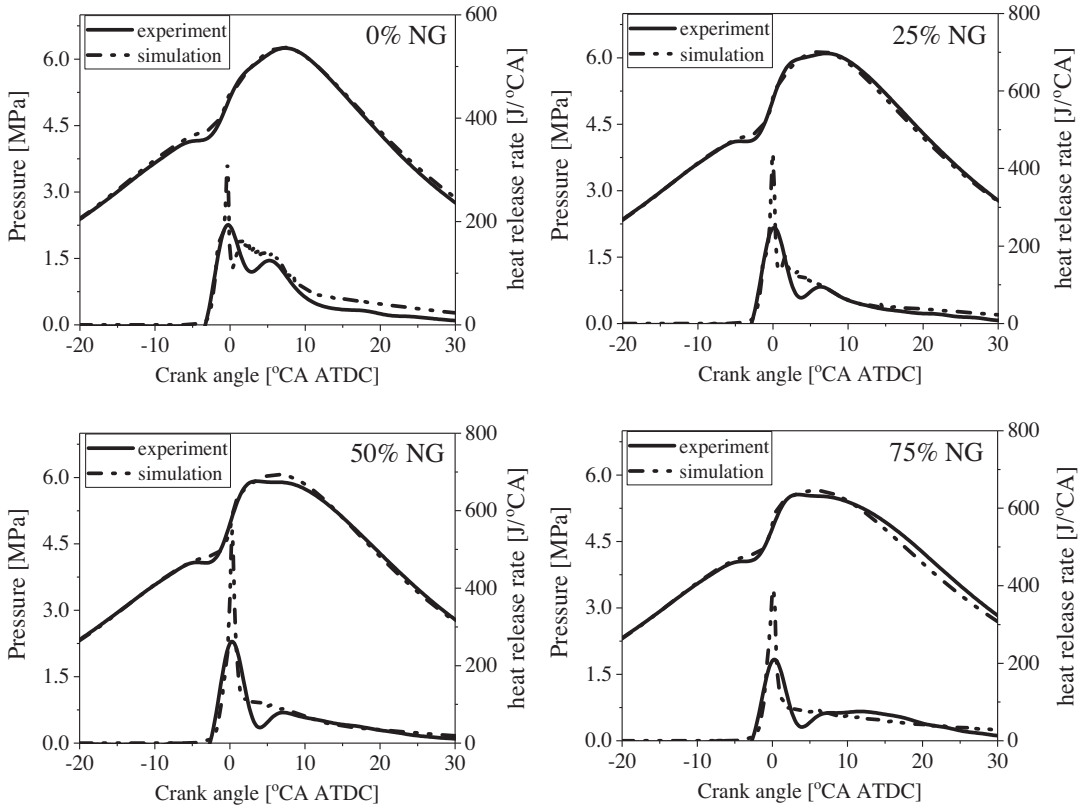

Fig. 2. Comparison of the simulated cylinder pressure and heat release rate with experimental data measured at 0%, 25%, 50%, and 75% NG, respectively.

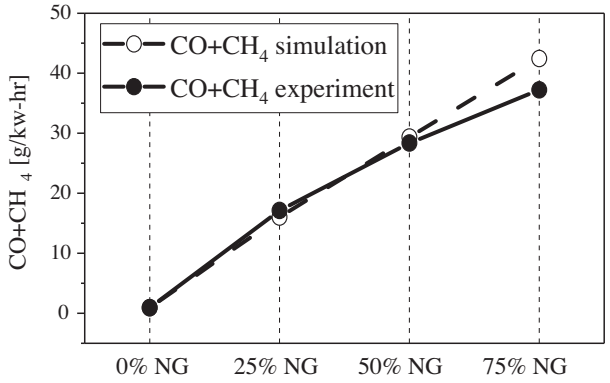

Fig. 4. Comparison of the sum of the simulated methane and CO with experimental data.

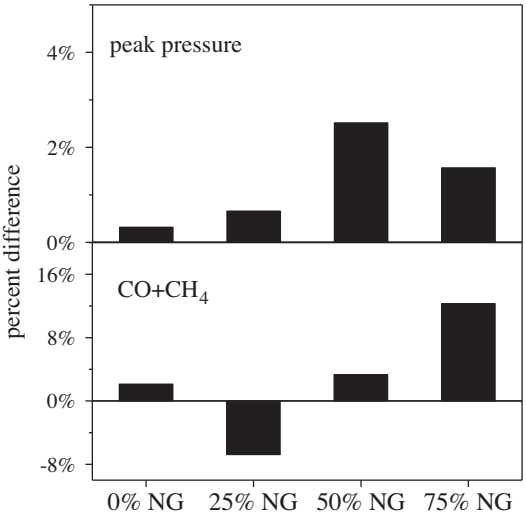

Fig. 5. Difference between the Predicted and Measured CO + CH_4 emissions and peak cylinder pressure.

leading to the oxidation of the unburned methane. This contributes to the combustion of methane presented outside the pilot fuel spray plume and the oxidation of the intermediate combustion products such as CO originating from rich combustion products because O_2 is made available from the O_2-rich methane-air mixture. Accordingly, the combustion of methane outside the spray plume is dominated by the mixing of the hot combustion products and the unburned methane-air mixture.

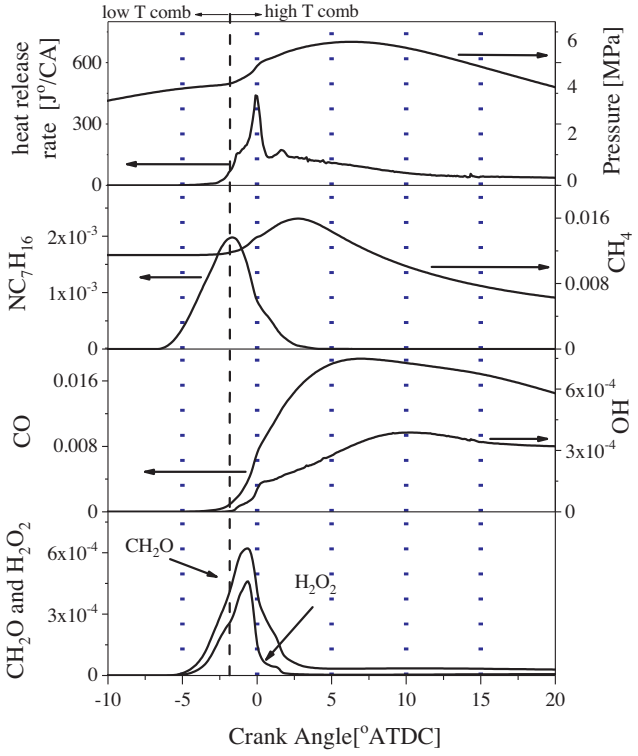

Fig. 7. Variation of cylinder pressure, heat release rate, and the molar fraction of n-Heptane, methane, CO, OH, H_2O_2, and CH_2O with changes in crank angle. Case: 25% NG.

Such a process is controlled by the interaction between piston compression, the bulk gas movement triggered by the pilot fuel spray jet, and expansion of combustion products due to the temperature increase during combustion. The bulk movement triggered by the spray jet and the subsequent mixing with the cool NG-air mixture, and oxidation of methane gradually become weak, especially after the completion of the main combustion process. This slows down the mixing of hot combustion products with the unburned mixture and the oxidation of methane present outside pilot fuel spray plume.

Fig. 9 shows the spatial distribution of O_2, methane and temperature of bulk gas at about 20 °CA ATDC representing the late diffusion combustion. The arrow vectors shown in the temperature distribution figure are the distribution of velocity representing the movement of bulk gas driven by the momentum of the pilot fuel, expansion of bulk gas due to combustion, and down-ward movement of the piston. The

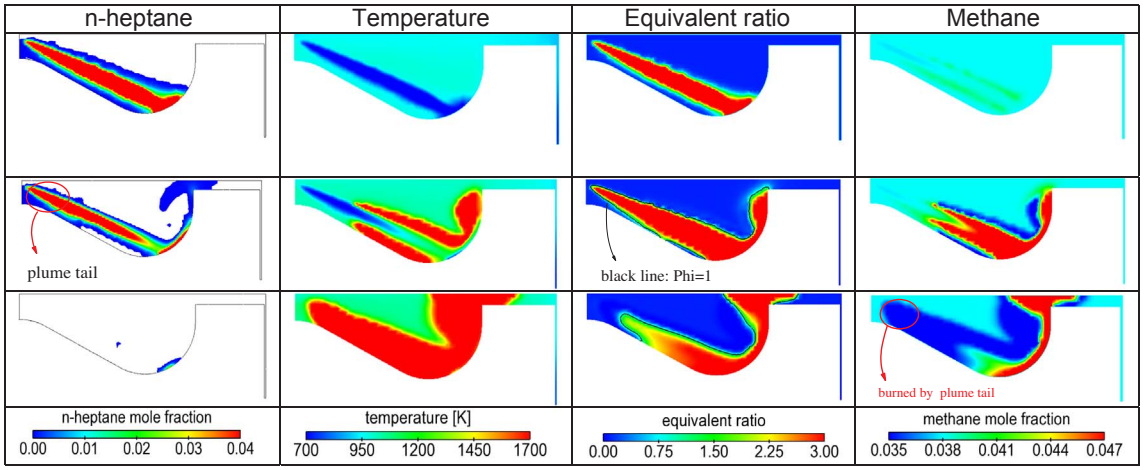

Fig. 6. The evolution of spray plume, distribution of temperature, equivalent ratio, and molar fraction of methane during n-heptane injection and ignition process. Case: 25%NG. From top to bottom: −2.5, 0.1, 4.3 CA ATDC.

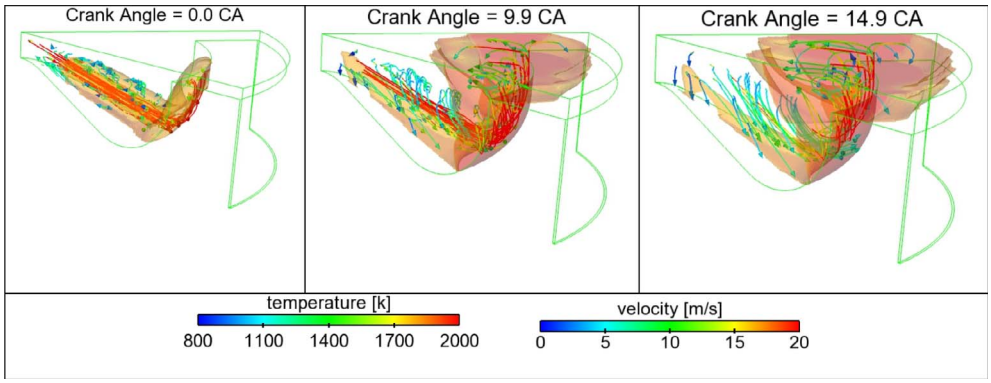

Fig. 8. The distribution of temperature and velocity at 0, 9.9, and 14.9 °CA ATDC. NG%25.

methane concentration in the vacant region (no color) surrounded by the dark blue one (representing low methane concentration) shown in the methane distribution figure is extremely low, indicating the complete combustion of methane. As shown in Fig. 9, the velocity field of the bulk gas observed in the 25% NG case is much stronger than that observed in the 75% NG case. This is due to the higher momentum of the pilot fuel injected at 25% NG than that at 75% NG benefiting from the injection of more pilot fuel at 25% NG than 75% NG. Accordingly, the hot combustion products at 25% NG are pushed further toward the cylinder head, the surface of combustion chamber, touch the piston bowl surface and bounce back toward the centerline of the combustion chamber. In comparison, the injection momentum in the 75% NG case is relatively too weak for the pilot fuel to reach the piston bowl surface, so it drives the hot combustion products toward the piston platform and the squish, resulting in methane/air consumption in a different region. The low O_2 concentration (dark blue and region without color surrounded by dark blue) shown in Fig. 9 represents the region where the combustion of n-heptane is involved as the majority of O_2 has been consumed by combustion. This is supported by the high bulk mixture temperature observed. The medium O_2 concentration area (light-blue and green) represents the region where combustion/oxidation of methane is involved or mixed with combustion products of pilot fuel. The methane in this region is consumed during the post combustion oxidation process after being mixed with hot combustion products. The methane concentrations in these two regions are extremely low as represented by the blue area. The region featuring a high concentration of O_2 and methane represents the bulk gas where the oxidation of methane has not been initiated or only partially oxidized. Plus, the addition of methane affects the mass of pilot fuel injected, the development of the pilot fuel spray, atomization, mixing with the bulk gas, and combustion. This is confirmed by the distribution of unburned methane in cylinder shown in Fig. 9. The addition of more NG decreases the volume of the region with unburned methane, which is due to the improved post combustion oxidation of methane. It is evident that the mixing of the hot combustion products with the unburned methane-air mixture to some extent dominates the consumption of methane in the premixed methane-air mixture without involving n-heptane.

The unburned methane observed in the dual fuel engine after the

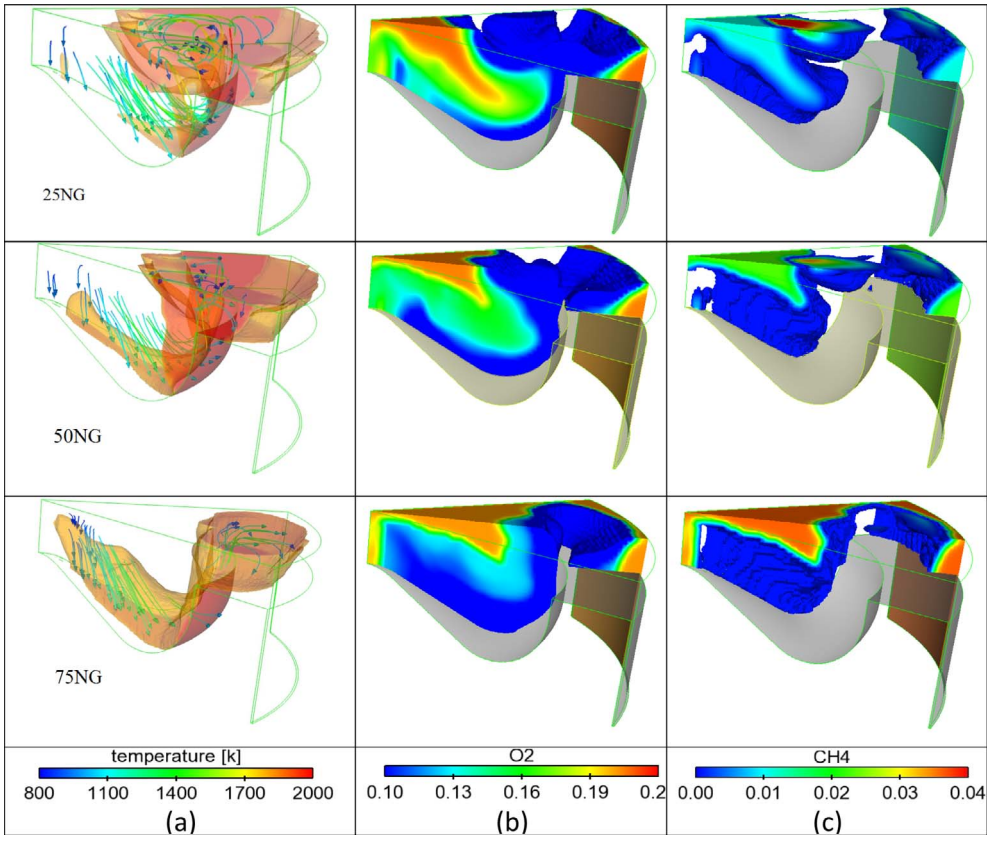

Fig. 9. The distribution of temperature and velocity, O_2 and CH_4 observed at 20 °CA ATDC. Case: 25%NG, 50%NG, and 75%NG.

completion of the main combustion process is located at a region away from the pilot fuel plume where the unburned methane-fuel mixture has not had a chance to be mixed with the hot combustion products. Fig. 10 shows the distribution of unburned methane, the bulk mixture temperature, and the velocity field in the interface region at 50 °CA ATDC representing a crank angle at which the post-combustion oxidation of methane becomes weak. The hot combustion products were moving downward following the downward movement of the piston. In comparison, the driving force originating from the injection of the pilot fuel and early combustion become negligible. The heat release at this stage is very low due to the slow oxidation of methane occurring at the interface between the hot combustion products and the relatively cool methane-air mixture. This is due to the very slow mixing between the hot combustion products and cool mixture containing methane. Plus, the temperature of the bulk gas in both the burned and unburned area is decreasing with the further downward movement of the piston. As shown in Fig. 10, the majority of methane survived is present in the area far from the hot combustion products. The majority of methane survived at this point will eventually exit the cylinder as unburned methane.

It is evident that the combustion of pilot fuel, volumetric ratio of the injection spray plume or pilot fuel vapor relative to the total volume,

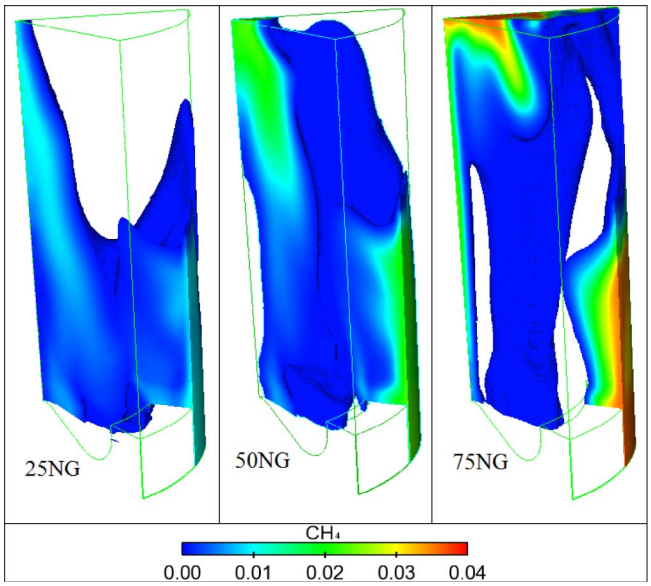

Fig. 11. Distribution of the unburned methane in cylinder at exhaust valve opening.

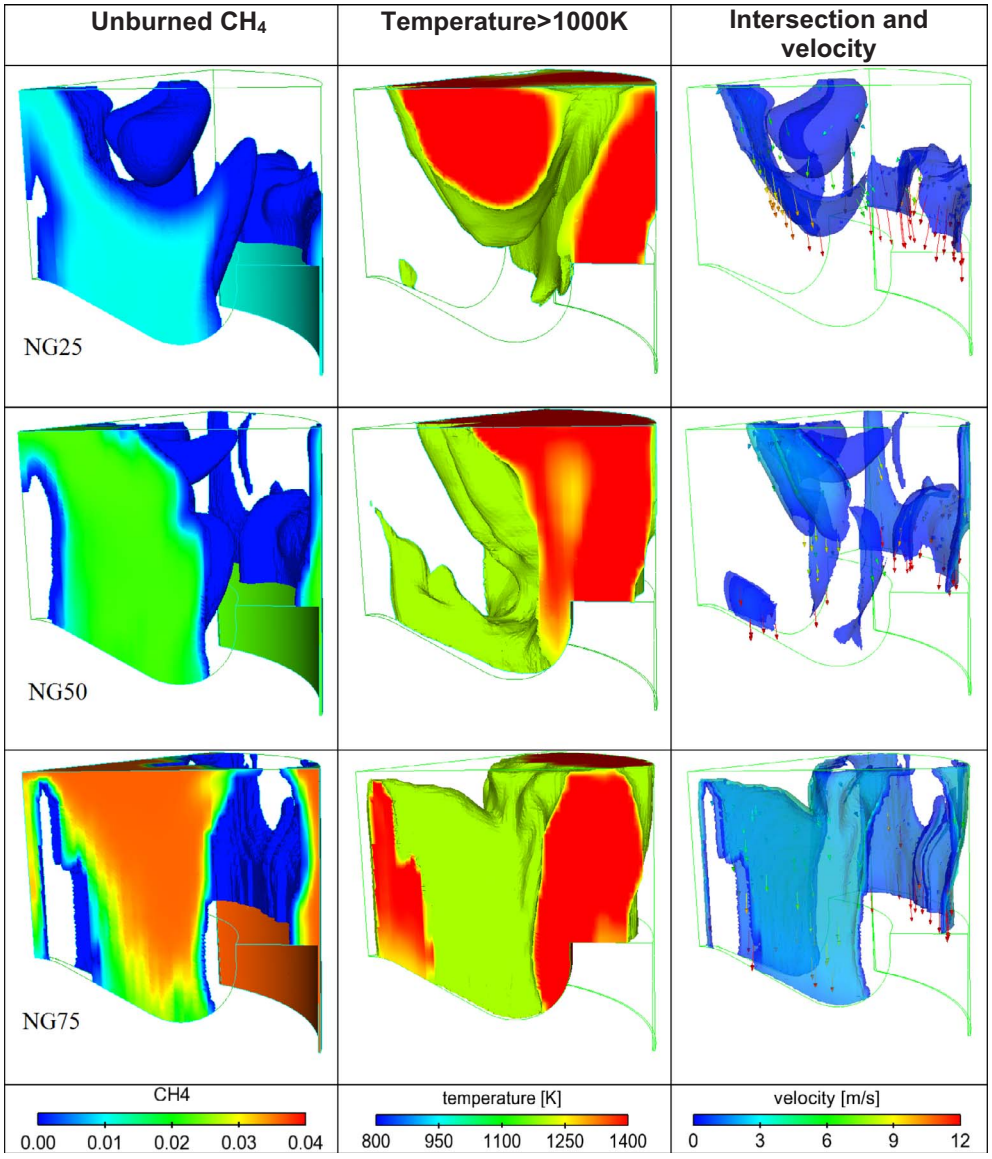

Fig. 10. Distribution of the unburned methane, bulk mixture temperature, and velocity field in the interface at 50 °CA ATD for 25%NG, 50%NG and 75%NG case.

the movement of the hot combustion products towards to unburned mixture, and its mixing with methane-air mixture dominate the combustion of methane in a dual fuel engine. The injection parameter of pilot fuel such as pressure, injection timing (affecting the pressure of bulk gas in-cylinder), geometry of injector holes, number of injector holes, and injection angle may play an important role in methane emissions from NG-diesel dual fuel engines at low loads when the concentration of methane is too low to support the propagation of the turbulent flame. This is consistent with experimental results observed in an optical engine [24,26].

Fig. 11 shows the distribution of methane in-cylinder at EVO. In this research, the methane observed at EVO is reported as the emissions of unburned methane. The unburned methane is mainly located at the n-heptane free region such as the center of the combustion chamber and boundary area around the cylinder liner, especially for the 50% NG and 75% NG cases. In comparison, the contribution of the boundary layer to total unburned methane is found to increase with increasing the amount of methane. The development of the approaches and control strategies in reducing the emissions of unburned methane should focus on enhancing the combustion of methane in the center of the combustion chamber.

4. Discussion

The simulated distribution of methane and its variation with combustion process is further processed to derive the percentage of methane consumed in each stage. Fig. 12 shows the percentage of methane consumed during each stage and the percentage of methane observed at EVO. The main combustion process consumed 43–53% of the methane followed by 17–29% consumption during the post combustion oxidation process. The unburned methane observed at EVO was about 27–35% of that added to the intake mixture at the simulated load. It should be noted that the combustion of methane is affected by the concentration of methane added, the volume of pilot fuel spray plume, the temperature of combustion products, and the mixing between the hot combustion products and pilot fuel-free bulk mixture containing methane. The mixing between the hot combustion products and pilot fuel-free bulk mixture containing methane is dominated by the movement of the hot combustion products. The movement of the hot bulk gas is initiated by the momentum of the pilot fuel directly injected into the cylinder, enhanced by the expansion of the combustion products due to the increased temperature during the combustion process, and guidance of the piston bowl. The interaction among pilot fuel, configuration of the combustion chamber, direction of piston movement, and combustion process dominate the mass transfer of the hot combustion products to the cold unburned methane-air mixture.

The simulation work conducted in this research reveals the combustion of methane in a dual fuel engine, the important role of post-combustion oxidation in burning the methane surviving the main combustion process, and the spatial distribution of the unburned methane in-cylinder. The optimization of the engine aiming to enhance the combustion of methane in a dual fuel engine should focus on the following aspects: (1) increasing the relative volumetric ratio of bulk gas mixed with vapors of the pilot fuel. This can be achieved through (i) modifying the design of the fuel injector such as increasing the size or volume of pilot fuel spray plume which can be achieved through the adjusting the spray angle, number of injection holes, and diameter of injector holes; (ii) Increasing the ignition delay time period to allow for enough time for the atomization, vaporization of pilot fuel, and its mixing with bulk gas prior to the auto-ignition of the pilot fuel vapor. This can be achieved through optimizing fuel injection strategies such as using multiple-fuel injection pules such as adding a mini-pilot injection pulse prior to the main injection pulse of pilot fuel. (2) Enhancing the movement of the hot bulk gas toward the cold unburned methane mixture, especially the movement of hot combustion products toward the center of the cylinder, which requests a better design of the piston bowl geometry. The mixing of the combustion products with the unburned premixed mixture should occur early in the expansion process when the temperature of the hot combustion products is still sufficiently high to oxidize the unburned methane.

5. Conclusion

A numerical study on the combustion of methane in a NG-diesel dual fuel engine during the main combustion and post combustion process has been conducted. The spatial distribution of methane in-cylinder and the consumption at each combustion stage are examined. Based on the methane combustion and distribution data simulated at the engine speed of 910 RPM and load of 4.05 bar bmep, the following conclusions can be drawn:

(1) The combustion of methane in a dual fuel engine at low loads is dominated by the combustion of pilot fuel, the relative volumetric ratio of pilot fuel vapor over the total volume, the movement of the hot combustion products towards the unburned mixture, and the mixing of the hot combustion products with the unburned methane-air mixture.
(2) The spray plume of the pilot fuel injected into the cylinder produced a high velocity field of the bulk gas under the guidance of the piston bowl shape, which helps the mixing of the hot combustion products with the unburned methane and contributes most to methane consumption during the combustion process. The main combustion process consumed 43–53% of the methane.
(3) The post-combustion oxidation of methane occurs in the interface between the hot combustion products and unburned pre-mixed mixture, which increases the temperature of methane to that needed for its oxidation. The post-combustion process consumes 17–29% of the methane.
(4) The unburned methane observed at EVO was located mainly at the center of the cylinder. The portion of methane present at the boundary layer near the cylinder liner is relatively small. The total methane left unburned at EVO was 27–35% of the intake methane.
(5) The optimization of dual fuel engine design, operation and fuel injection strategies aiming to minimize methane emissions should focus on those capable of increasing the relative volume of pilot fuel vapor or its combustion products, or increasing the chance for the unburnt methane to mix with hot combustion products early in the expansion process when the temperature of the combustion products is still high.

The model validated in this research will be applied to develop the fuel injection strategies aiming to minimize the emissions of methane. The design of the fuel injection system and combustion chamber geometry can also be optimized using this CFD platform.

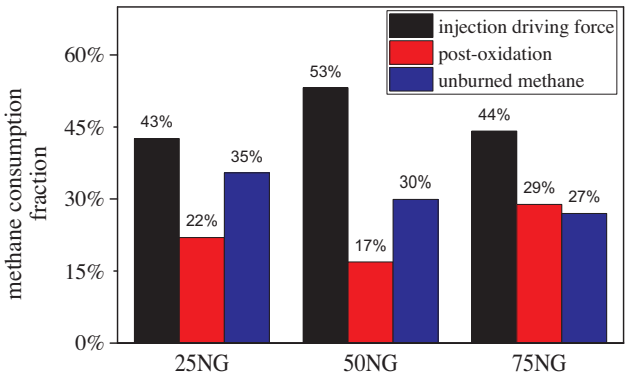

Fig. 12. Methane consumption during each stage after 99% n-heptane consumed.

Acknowledgement

This project is funded by US Department of Energy (Contract Number DE-FE0013689). The support of Convergent Science toward this research is gratefully appreciated. The author acknowledges the funding support provided by Natural Resources Canada through the PERD Energy End Use (project 3B03.003) and National Research Council Canada through the internal Bioenergy Program.

References

[1] Vermiglio E, Jenkins T, Kieliszewski M, Lapetz J, et al. Ford's SULEV dedicated natural gas trucks. SAE Technical Paper 1997;971662. http://dx.doi.org/10.4271/971662.
[2] Cho HM, He B. Spark ignition natural gas engines—a review. J Energy Convers Manage 2007;48(2):608–18. http://dx.doi.org/10.1016/j.enconman.2006.05.023.
[3] Karim GA. Combustion in gas fueled compression: ignition engines of the dual fuel type. J Eng Gas Turbines Power 2003;125(3):827–36.
[4] Sahoo BB, Sahoo N, Saha UK. Effect of engine parameters and type of gaseous fuel on the performance of dual-fuel gas diesel engines—a critical review. J Renew Sustain Energy Rev 2009;13(6):1151–84.
[5] Papagiannakis RG, Hountalas DT. Combustion and exhaust emission characteristics of a dual fuel compression ignition engine operated with pilot diesel fuel and natural gas. Energy Convers Manage 2004;45(18):2971–87.
[6] Papagiannakis RG, Rakopoulos CD, Hountalas DT, Rakopoulos DC. Emission characteristics of high speed, dual fuel, compression ignition engine operating in a wide range of natural gas/diesel fuel proportions. Fuel 2010;89(7):1397–406.
[7] Egúsquiza JC, Braga SL, Braga CVM. Performance and gaseous emissions characteristics of a natural gas/diesel dual fuel turbocharged and aftercooled engine. J Braz Soc Mech Sci Eng 2009;31(2):142–50.
[8] Abd Alla GH, Soliman HA, Badr OA, Abd Rabbo MF. Effect of pilot fuel quantity on the performance of a dual fuel engine. Energy Convers Manage 2000;41(6):559–72.
[9] Bdelaal MM, Hegab AH. Combustion and emission characteristics of a natural gas-fueled diesel engine with EGR. Energy Convers Manage 2012;64:301–12.
[10] Lin Z, Su W. A study on the determination of the amount of pilot injection and rich and lean boundaries of the pre-mixed CNG/air mixture for a CNG/diesel dual-fuel engine. SAE Paper 2003-01-0765; 2003.
[11] Kusakaa J, Okamotob T, Daishoa Y, Kiharac R, Saito T. Combustion and exhaust gas emission characteristics of a diesel engine dual-fueled with natural gas. JSAE Rev 2000;21(4):489–96.
[12] Yang B, Wei X, Xi C, Liu Y, Zeng K, Lai M. Experimental study of the effects of natural gas injection timing on the combustion performance and emissions of a turbocharged common rail dual-fuel engine. Energy Convers Manage 2014;87:297–304.
[13] Abd Alla GH, Soliman HA, Badr OA, Abd Rabbo MF. Effect of injection timing on the performance of a dual fuel engine. Energy Convers Manage 2002;43(2):269–77.
[14] Liu J, Yang H, Wang H, Ouyang M, Hao S. Effects of pilot fuel quantity on the emissions characteristics of a CNG/diesel dual fuel engine with optimized pilot injection timing. Appl Energy 2013;110:201–6.
[15] Ryu K. Effects of pilot injection timing on the combustion and emissions characteristics in a diesel engine using biodiesel–CNG dual fuel. Appl Energy 2013;111:721–30.
[16] Ryu K. Effects of pilot injection pressure on the combustion and emissions characteristics in a diesel engine using biodiesel–CNG dual fuel. Energy Convers Manage 2013;76:506–16.
[17] Yang B, Xi C, Zeng K, Wei X, Zeng K, Lai M. Parametric investigation of natural gas port injection and diesel pilot injection on the combustion and emissions of a turbocharged common rail dual-fuel engine at low load. Appl Energy 2015;143:130–7.
[18] Clark N, McKain D, Johnson DR, Wayne S, Li H, Akkerman V, Sandoval C, Covington A, Mongold R, Hailer J, Ugarte OJ. Pump-to-wheels methane emissions from the heavy-duty transportation sector. Environ Sci Technol 2017;51:968–76.
[19] López JM, Gómez Á, Aparicio F, Sánchez FJ. Comparison of GHG emissions from diesel, biodiesel and natural gas refuse trucks of the City of Madrid. Appl Energy 2009;86:610–5.
[20] Graham LA, Rideout G, Rosenblatt D, Hendren J. Greenhouse gas emissions from heavy-duty vehicles. Atmos Environ 2008;42:4665–81.
[21] Karim GA. An examination of some measures for improving the performance of gas fuelled diesel engines at light load. SAE Paper 912366; 1991.
[22] Karim GA, Liu Z, Jones W. Exhaust emissions from dual fuel engines at light load. SAE Paper 932822; 1993.
[23] Gatts T, Liu S, Liew C, Ralston B, Bell C, Li H. An experimental investigation of incomplete combustion of gaseous fuels of a heavy-duty diesel engine supplemented with hydrogen and natural gas. Int J Hydrogen Energy 2009;37:7848–59.
[24] Dronniou N, Kashdan J, Lecointe B, Sauve K, et al. Optical investigation of dual-fuel CNG/diesel combustion strategies to reduce CO_2 emissions. SAE Int J Eng 2014;7(2):873–87. http://dx.doi.org/10.4271/2014-01-1313.
[25] Bade Shrestha SO, Karim GA. The operational mixture limits in engines fueled with alternative gaseous fuels. J Energy Res Technol 2016;128(3):223–8.
[26] Nithyanandan K, Gao Y, Wu H, Lee C, et al. An optical investigation of multiple diesel injections in CNG/diesel dual-fuel combustion in a light duty optical diesel engine. SAE Technical Paper 2017-01-0755; 2017. doi: 10.4271/2017-01-0755.
[27] Liu S, Li H, Gatts T, Liew C, Wayne S, Thompson G, Clark N, Nuszkowski J. An investigation of NO_2 emissions from a heavy-duty diesel engine fumigated with H_2 and natural gas. Combust Sci Technol 2012;184(12):2008–35.
[28] Wannatong K, Akarapanyavit N, Siengsanorh S, Chanchaona S. Combustion and knock characteristics of natural gas diesel dual fuel engine. SAE Technical Paper 2007-01-2047; 2007, doi: 10.4271/2007-01-2047.
[29] Liu C, Karim GA, Xiao F, Sohrabi A. An experimental and numerical investigation of the combustion characteristics of a dual fuel engine with a swirl chamber. SAE Technical Paper 2007-01-0615; 2007.
[30] Nieman DE, Dempsey AB, Reitz RD. Heavy-duty RCCI operation using natural gas and diesel. SAE Paper 2012-01-0379; 2012.
[31] Maghbouli A, Saray RK, Shafee S, Ghafouri J. Numerical study of combustion and emission characteristics of dual-fuel engines using 3D-CFD models coupled with chemical kinetics. Fuel 2013;106:98–105.
[32] Paykani A, Kakaee AH, Rahnama P, Reitz RD. Effects of diesel injection strategy on natural gas/diesel reactivity controlled compression ignition combustion. Energy 2015;90:814–26.
[33] Guo H, Neill, WS, Liko B. An experimental investigation on the combustion and emissions performance of a natural gas–diesel dual fuel engine at low and medium loads. ASME 2015 Internal Combustion Engine Division Fall Technical Conference. American Society of Mechanical Engineers; 2015.
[34] Richards KJ, Senecal PK, Pomraning ECONVERGE, (v2.3). Convergent Science. WI: Madison; 2015.
[35] Ra Y, Reitz RD. A reduced chemical kinetic model for IC engine combustion simulations with primary reference fuels. Combust Flame 2008;155(4):713–38.
[36] Yang B, Yao M, Cheng W, Li Y, Zheng J, Li S. Experimental and numerical study on different dual-fuel combustion modes fuelled with gasoline and diesel. Appl Energy 2014;113:722–33.
[37] O'Rourke PJ, Amsden AA. A spray/wall interaction submodel for the KIVA-3 wall film model. SAE Paper 2000-01-0271; 2000.
[38] Beale JC, Reitz RD. Modeling spray atomization with the Kelvin-Helmholtz/Rayleigh-Taylor hybrid model. Atom Sprays 1999;9:623–50.
[39] Schmidt DP, Rutland CJ. A new droplet collision algorithm. J Comput Phys 2000;164:62–80.
[40] Han Z, Reitz RD. Turbulence modeling of internal combustion engines using RNG κ-ε models. Combust Sci Technol 1995;106(4-6):267–95.